Stereoselectivity in Organometallic Reactions: Oxidative Addition of Alkyl Halides to Platinum(II)

Cliff R. Baar, Hilary A. Jenkins, Jagadese J. Vittal, Glenn P. A. Yap, and Richard J. Puddephatt*

Department of Chemistry, The University of Western Ontario, London, Ontario, Canada N6A 5B7

Received February 2, 1998

The ligands *cis*- and *trans*-1,2-(N=CHC$_6$H$_5$)$_2$C$_6$H$_{10}$ (*trans*, **1**; *cis*, **2**) underwent cyclometalation of one phenyl substituent on reaction with [Pt$_2$Me$_4$(μ-SMe$_2$)$_2$] (**3**) to give CH$_4$ and chiral platinum(II) complexes [PtMe{1-(N=CHC$_6$H$_4$)-2-(N=CHC$_6$H$_5$)C$_6$H$_{10}$}], containing new N,N,C-donor tridentate ligands (*trans*, **4**; *cis*, **5**); complex **4** was structurally characterized. Reaction of racemic **4** and **5** with primary alkyl halides (iodomethane, iodoethane, 1-iodopropane, and benzyl bromide) gave platinum(IV) products by oxidative addition, often with a high degree of stereoselectivity. The absolute configuration of the major stereoisomer was determined for the following representative platinum(IV) products by X-ray crystal structure analyses: [PtIMe$_2${*cis*-1-(N=CHC$_6$H$_4$)-2-(N=CHC$_6$H$_5$)C$_6$H$_{10}$}] (**7a**), [PtIMeEt{*trans*-1-(N=CHC$_6$H$_4$)-2-(N=CHC$_6$H$_5$)C$_6$H$_{10}$}] (**8a**), and [PtBrMeBz{*trans*-1-(N=CHC$_6$H$_4$)-2-(N=CHC$_6$H$_5$)C$_6$H$_{10}$}] (**13a**; Bz = benzyl). In other cases, structural assignment was made by NMR (including NOE effects in selected cases) and supported by molecular mechanics calculations. The first step of the oxidative addition occurs primarily at the face *syn* and *anti* to the cyclohexyl group in **4** and **5**, respectively, and the initial oxidative addition is *trans*. In the case of methyl iodide addition, but in no others, subsequent isomerization can occur to give products which appear to arise from *cis* oxidative addition, and the basis for this trend is elucidated. Hydrolysis of [PtIMeEt{*cis*-1-(N=CHC$_6$H$_4$)-2-(N=CHPh)C$_6$H$_{10}$}] (**9b**) gives PhCH=O and [PtIMeEt{*cis*-1-(N=CHC$_6$H$_4$)-2-(NH$_2$)C$_6$H$_{10}$}], with a change in stereochemistry at platinum.

Downloaded by CARLI CONSORTIUM on June 30, 2009
Published on May 23, 1998 on http://pubs.acs.org | doi: 10.1021/om980065z

Introduction

Since the oxidative addition of alkyl halides to transition-metal complexes is a key step in several important catalytic reactions,[1] there have been many studies to determine the scope of the reaction and to study reactivity and mechanism.[1−5] In most cases, the oxidative addition of primary alkyl halides to dimethylplatinum(II) complexes occurs by the polar S$_N$2 mechanism and gives *trans* stereochemistry,[1,3−5] though subsequent isomerization can give products which appear to arise from *cis* oxidative addition, as illustrated in eq 1.[6]

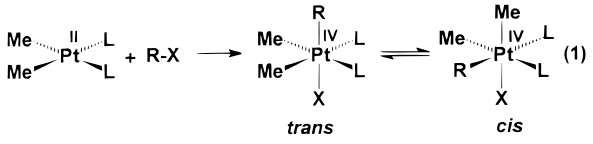

LL = bipy, R-X = MeI, BzBr

Surprisingly little attention has been placed on the potential stereoselectivity of oxidative addition of alkyl halides to square-planar complexes having no plane of symmetry in the molecular plane.[2] This paper reports such a study, using platinum(II) complexes with metalated diimine ligands derived from *cis*- or *trans*-diaminocyclohexane, which naturally give chiral products.[7] It will be shown that the oxidative-addition reactions occur with high stereoselectivity, and that the presence of asymmetry can lead to a more complex sequence of steps in the oxidative addition than is normally observed. It has previously been shown that similar diimine ligands containing 2-halogenoaryl substituents give highly stereoselective intramolecular oxidative additions of the aryl−halogen bonds to platinum(II)[8] and that similar ligands are useful in chiral catalysis.[9]

Results

Synthesis and Characterization of Ligands. The Schiff base ligand *trans*-1,2-(N=CHC$_6$H$_5$)$_2$C$_6$H$_{10}$ (**1**) was

(1) Stille, J. K. *The Chemistry of the Metal−Carbon Bond*; Hartley, F. R., Patai, S., Eds.; Wiley: New York, 1985; Vol. 2, Chapter 9.

(2) (a) Gianini, M.; Forster, A.; Haag, P.; Stoeckli-Evans, H. *Inorg. Chem.* **1996**, *35*, 4889. (b) Wehman-Ooyevaar, I.; Drenth, W.; Grove, D. M.; van Koten, G. *Inorg. Chem.* **1993**, *32*, 3347.

(3) (a) Jawad, J. K.; Puddephatt, R. J. *J. Organomet. Chem.* **1976**, *117*, 297. (b) Jawad, J. K.; Puddephatt, R. J. *J. Chem. Soc., Dalton Trans.* **1977**, 1466. (c) Monaghan, P. K.; Puddephatt, R. J. *Organometallics* **1986**, *5*, 439. (d) Crespo, M.; Puddephatt, R. J. *Organometallics* **1987**, *6*, 2548. (e) Monaghan, P. K.; Puddephatt, R. J. *J. Chem. Soc., Dalton Trans.* **1988**, 595.

(4) Brown, M. P.; Puddephatt, R. J.; Upton, C. E. E. *J. Chem. Soc., Dalton Trans.* **1974**, 2457.

(5) (a) Monaghan, P. K.; Puddephatt, R. J. *Organometallics* **1985**, *4*, 1406. (b) Scott, J. D.; Puddephatt, R. J. *Organometallics* **1986**, *5*, 1538.

(6) (a) von Zelewsky, A.; Suckling, A. P.; Stoeckli-Evans, H. *Inorg. Chem.* **1993**, *32*, 4585. (b) Achar, S.; Scott, J. D.; Puddephatt, R. J. *Polyhedron* **1996**, *15*, 2363.

(7) For chirality descriptors see: Block, B. P.; Powell, W. H.; Fernelius, W. C. *Inorganic Chemical Nomenclature: Principles and Practice*; American Chemical Society: Washington, DC, 1990; Chapter 16.

S0276-7333(98)00065-X CCC: $15.00 © 1998 American Chemical Society
Publication on Web 05/23/1998

Scheme 1

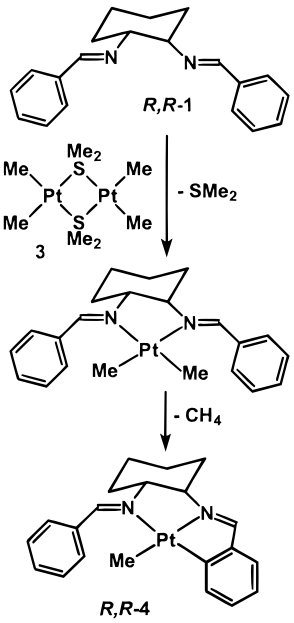

Scheme 2

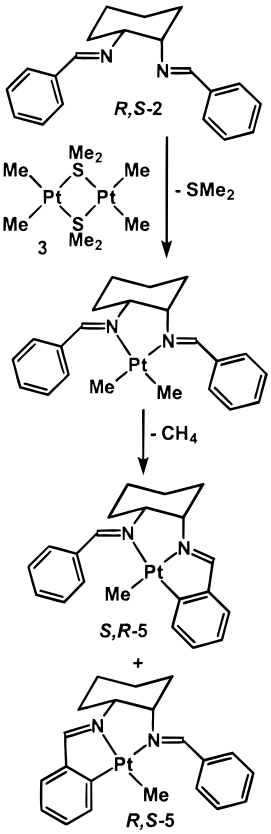

prepared by the condensation of racemic (*R*,*R*,*S*,*S*)-*trans*-1,2-diaminocyclohexane with benzaldehyde in the presence of $MgSO_4$. The meso (*R*,*S*) ligand *cis*-1,2-$(N{=}CHC_6H_5)_2C_6H_{10}$ (**2**) was prepared similarly. The ligands were formed as single isomers, and *anti* stereochemistry is assumed about each imine N=CH bond and has been confirmed in several complexes derived from them. The complexes were fully characterized using ^1H NMR spectroscopy and either microanalysis or high-resolution mass spectroscopy.

Racemic [PtMe{*trans*-1-(N=CHC$_6$H$_4$)-2-(N=CHC$_6$H$_5$)C$_6$H$_{10}$}] (4) and Racemic [PtMe{*cis*-1-(N=CHC$_6$H$_4$)-2-(N=CHC$_6$H$_5$)C$_6$H$_{10}$}], (5). The ligands *trans*- and *cis*-1,2-$(N{=}CHC_6H_5)_2C_6H_{10}$ (**1** and **2**) each reacted with $[Pt_2Me_4(\mu\text{-}SMe_2)_2]$ (**3**) to give, not the simple diimine complexes expected to arise from ligand substitution, but the products of cycloplatination [PtMe{1-(N=CHC$_6$H$_4$)-2-(N=CHC$_6$H$_5$)C$_6$H$_{10}$}] (*trans*, **4**; *cis*, **5**), with corresponding loss of CH_4 (Schemes 1 and 2).[10] These reactions are expected to proceed by ligand substitution to give the corresponding dimethyl(diimine)platinum(II) complex (Schemes 1 and 2) followed by intramolecular oxidative addition of an aryl C−H bond to give a platinum(IV) intermediate which undergoes reductive elimination of methane.[10,11] However, these proposed intermediates are not detectable and only the final products **4** and **5** were characterized. Though stereoselectivity is expected in the oxidative-addition step, no useful information is obtained.

Scheme 1 shows only the reaction derived from (*R*,*R*-**1**, and metalation of either phenyl substituent gives the same product *R*,*R*-**4**; racemic **1** thus gives racemic **4**. The case of the meso ligand **2** is somewhat more complex, but the two phenyl groups are chemically identical and reaction naturally gives equal amounts of the enantiomeric products *S*,*R*-**5** and *R*,*S*-**5** (the nomenclature used places the descriptor for the higher priority chiral carbon atom, the one connected to the metalated aryl group, first). Thus, the meso ligand **1** gives the racemic product **5**. The spectroscopic properties of the complexes are fully consistent with these predictions. Thus, the ^1H NMR spectra of complexes **4** and **5** (Table 1) each contained a single methylplatinum resonance with coupling constant $^2J(PtH) = 83$ Hz for **4** and 84 Hz for **5**, typical of platinum(II) methyl groups *trans* to N-donors.[10,12] The ^1H NMR spectra of **4** and **5** also show the characteristic ^{195}Pt satellites on the imine proton resonances (Table 1).

Complex **4** was also characterized by an X-ray structure determination; selected bond distances and angles are given in Table 2, and a view of the structure of the *S*,*S* isomer is shown in Figure 1. The structure establishes the presence of the tridentate N,N,C-donor ligand formed by metalation of one of the phenyl substituents of the ligand **1** and shows that the platinum(II) center has square-planar geometry. The angles at platinum are distorted due to the constraints of the tridentate

(8) Baar, C. R.; Hill, G. S.; Vittal, J. J.; Puddephatt, R. J. *Organometallics* **1998**, *17*, 32.

(9) (a) Omae, I. *Chem. Rev.* **1979**, *79*, 287. (b) Constable, E. C. *Polyhedron* **1984**, *3*, 1037. (c) Ryabov, A. D. *Synthesis* **1985**, 233. (d) Newkome, G. R.; Puckett, W. E.; Gupta, C. K.; Kiefer, G. E. *Chem. Rev.* **1986**, *86*, 451.

(10) (a) Anderson, C. M.; Ferguson, G.; Lough, A. J.; Puddephatt, R. J. *J. Chem. Soc., Chem. Commun.* **1989**, *18*, 1297. (b) Anderson, C. M.; Crespo, M.; Jennings, M. C.; Lough, A. J.; Ferguson, G.; Puddephatt, R. J. *Organometallics* **1991**, *10*, 2672. (c) Perera, S. D.; Shaw, B. L. *J. Chem. Soc., Dalton Trans.* **1995**, 641. (d) Crespo, M. *Polyhedron* **1996**, *15*, 1981. (e) Crespo, M.; Solans, X.; Font-Bardia, M. *J. Organomet. Chem.* **1996**, *518*, 105.

(11) (a) Poss, M. J.; Arif, A. M.; Richmond, T. G. *Organometallics* **1988**, *7*, 1669. (b) Richmond, T. *Coord. Chem. Rev.* **1990**, *105*, 221. (c) Crespo, M.; Martinez, M.; Sales, J. *J. Chem. Soc., Chem. Commun.* **1992**, 882. (d) Anderson, C. M.; Crespo, M.; Ferguson, G.; Lough, A. J.; Puddephatt, R. J. *Organometallics* **1992**, *11*, 1177. (e) Kiplinger, J. L.; King, M. A.; Fechtenkotter, A.; Arif, A. M.; Richmond, T. G. *Organometallics* **1996**, *15*, 5292.

(12) (a) Scott, J. D.; Puddephatt, R. J. *Organometallics* **1983**, *2*, 1645. (b) Kuyper, J. *Inorg. Chem.* **1977**, *16*, 2171.

Downloaded by CARLI CONSORTIUM on June 30, 2009
Published on May 23, 1998 on http://pubs.acs.org | doi: 10.1021/om980065z

Table 1. ^{1}H NMR Data (300 MHz in CD_2Cl_2 Solution) for MePt and N=CH Groups in Complexes 4−14

	N−Pt−Me		X−Pt−Me		N=CH	
complex	δ	^2J(PtH)/Hz	δ	^2J(PtH)/Hz	δ	^3J (PtH)/Hz
4	0.51	83			8.64	61
					8.98	47
5	0.61	84			8.69	63
					9.02	45
6a	0.78	67	0.67	71	8.51	50
					8.82	36
6b	0.95	66	0.66	72	8.49	49
					8.96	36
7a[a]	0.87	66	0.82	72	8.55	49
					8.84	34
7b[a]	0.87	67	0.65	71	8.51	
					8.83	
8a	0.74	67	*b*		8.53	52
					8.88	39
9b	0.87	67	*b*		8.51	52
					8.85	38
10	*b*		0.93	72	8.37	44
11a	0.79	66	*c*		8.47	49.5
					8.83	39
12b	0.89	67	*c*		8.51	51
					8.85	38
13a	0.77	66	*d*		8.43	51
					8.71	38
13b	1.01	66	*d*		8.08	53
					9.06	37
14b	0.86	66	*d*		8.40	51
					8.76	37

[a] Solvent $CDCl_3$. [b] Et group here. [c] Pr group here. [d] Bz group here.

Table 2. Selected Bond Distances and Angles for Complex 4

(a) Bond Distances (Å)			
Pt(1)−C(2)	2.01(1)	Pt(1)−N(1)	2.06(1)
Pt(1)−C(1)	2.08(1)	Pt(1)−N(2)	2.12(1)
N(1)−C(8)	1.28(1)	N(1)−C(9)	1.46(1)
N(2)−C(15)	1.29(1)	N(2)−C(14)	1.48(1)
C(2)−C(7)	1.39(1)	C(7)−C(8)	1.44(1)
C(9)−C(14)	1.55(1)	C(15)−C(16)	1.49(1)
(b) Bond Angles (deg)			
C(2)−Pt(1)−N(1)	80.9(4)	C(2)−Pt(1)−C(1)	96.5(4)
N(1)−Pt(1)−C(1)	171.7(4)	C(2)−Pt(1)−N(2)	161.7(4)
N(1)−Pt(1)−N(2)	80.8(3)	C(1)−Pt(1)−N(2)	101.5(4)
C(8)−N(1)−Pt(1)	113.6(7)	C(9)−N(1)−Pt(1)	115.0(7)
C(14)−N(2)−Pt(1)	104.5(6)	C(7)−C(2)−Pt(1)	111.5(8)
C(2)−C(7)−C(8)	116.5(9)	N(1)−C(8)−C(7)	117.1(9)
N(1)−C(9)−C(14)	105.9(8)	N(2)−C(14)−C(9)	109.1(8)

ligand, with N(1)−Pt−N(2) and N(1)−Pt−C(2) less than 90° and C(1)−Pt−N(2) and C(1)−Pt−C(2) greater than 90° (Table 2). The stereochemistry at both imine groups is *anti*, and the cyclohexane ring has the chair conformation, as expected. All the bond distances are in the expected ranges, once allowance is made for the strong *trans* influence of the carbon donors.[13]

The complexes **4** and **5** are stable but electron-rich chiral platinum(II) complexes and so are clearly suitable substrates for the study of stereoselectivity in oxidative addition. The oxidative addition of the reagent R−X to **4** or **5** could give many isomeric platinum(IV) products. However, the number will be limited to four for a given enantiomer of **4** or **5**, given the constraints imposed by the tridentate ligand having a strong preference for

(13) For example, see: (a) Clegg, D. E.; Hall, J. R.; Swile, G. A. *J. Organomet. Chem.* **1972**, *38*, 403. (b) Hill, G. S.; Vittal, J. J.; Puddephatt, R. J. *Organometallics* **1997**, *16*, 1209.

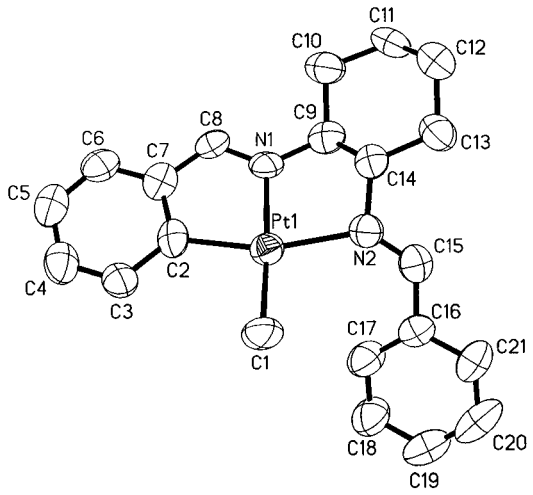

Figure 1. View of the structure of the *S,S* enantiomer of complex **4**.

Chart 1. Oxidative Addition to 4

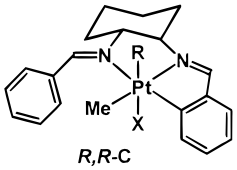

R,R-C

6a, R = Me, X = I
6a*, R = CD_3, X = I
8a, R = Et, X = I
11a, R = Pr, X = I
13a, R = Bz, X = Br

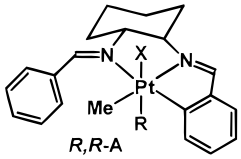

R,R-A

6b, R = Me, X = I
6b*, R = CD_3, X = I
8b, R = Et, X = I
11b, R = Pr, X = I
13b, R = Bz, X = Br

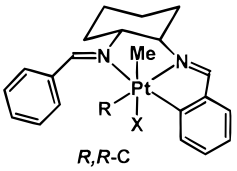

R,R-C

6c, R = Me, X = I
6c*, R = CD_3, X = I
8c, R = Et, X = I
11c, R = Pr, X = I
13c, R = Bz, X = Br

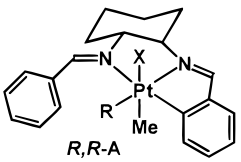

R,R-A

6d, R = Me, X = I
6d*, R = CD_3, X = I
8d, R = Et, X = I
11d, R = Pr, X = I
13d, R = Bz, X = Br

meridional coordination and the platinum(IV) center having a strong preference for the facial coordination of the three carbon donor ligands.[3−6,8,10] The possible isomers are then shown as **a**−**d** in Charts 1 and 2. The R−X groups may add *trans* to give **a** and **b** or *cis* to give **c** and **d**. For each stereochemistry of R−X addition to **4**, there are two possible diastereomers defined in Chart 1 as *R,R-C* and *R,R-A* (also *S,S-C* and *S,S-A* for the racemic ligand, with *C* and *A* defining the chirality at platinum(IV)) since the methyl group of MeI can approach and add to either of the two distinct faces of the chiral square-planar complex during the oxidative addition, thus giving the isomers **a**,**b** or **c**,**d**. Oxidative addition to **5** gives similar results except that the diastereomeric pairs have the chirality descriptors *S,R-A* and *S,R-C* (and *R,S-C* and *R,S-A* since **5** is racemic) as shown in Chart 2. Reactions have been studied with R−X = MeI, CD_3I, EtI, PrI, and BzBr (Bz = $PhCH_2$), and these are described sequentially below.

Oxidative Addition of Methyl Iodide. Racemic [PtMe{*trans*-1-(N=CHC_6H_4)-2-(N=CHC_6H_5)C_6H_{10}}] (**4**) reacted quickly with iodomethane in THF at room

Downloaded by CARLI CONSORTIUM on June 30, 2009
Published on May 23, 1998 on http://pubs.acs.org | doi: 10.1021/om980065z

Chart 2. Oxidative Addition to 5

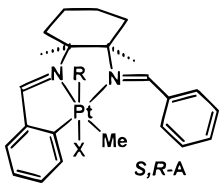

7a, R = Me, X = I
7a*, R = CD_3, X = I
9a, R = Et, X = I
12a, R = Pr, X = I
14a, R = Bz, X = Br

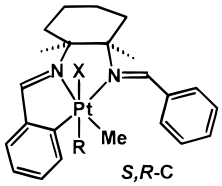

7b, R = Me, X = I
7b*, R = CD_3, X = I
9b, R = Et, X = I
12b, R = Pr, X = I
14b, R = Bz, X = Br

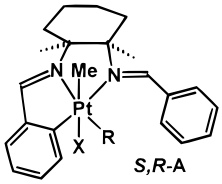

7c, R = Me, X = I
7c*, R = CD_3, X = I
9c, R = Et, X = I
12c, R = Pr, X = I
14c, R = Bz, X = Br

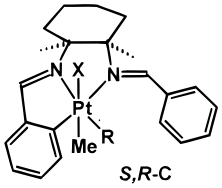

7d, R = Me, X = I
7d*, R = CD_3, X = I
9d, R = Et, X = I
12d, R = Pr, X = I
14d, R = Bz, X = Br

temperature to give a mixture of two diastereomers of the platinum(IV) complex [$PtIMe_2${*trans*-1-(N=CHC_6H_4)-2-(N=CHC_6H_5)C_6H_{10}}] (**6**). Note that, in this case with R = Me, the isomers **6a**,**c** and **6b**,**d** are structurally equivalent; therefore, only two isomers are possible and two are observed.

The presence of two diastereomers was established from the ^{1}H NMR spectra of the complexes (Table 1), obtained as soon as possible after isolation so as to minimize possible complications due to isomerization after the initial oxidative addition. The major diastereomer, subsequently assigned the structure **6a** (or **6c**), gave resonances at δ 0.67, ^2J(PtH) = 71 Hz and δ 0.78, ^2J(PtH) = 67 Hz, assigned to the methylplatinum groups *trans* to iodide and the imine group, respectively. This is consistent with previous work involving similar platinum(IV) complexes, in which it was shown that methylplatinum resonances *trans* to an iodide ligand occurred at lower frequency than those *trans* to a nitrogen donor and have a somewhat higher value of ^2J(PtH) due to the low *trans* influence of iodide.[3d,5a,14] The magnitude of the ^2J(PtH) coupling constants are diagnostic of a platinum(IV) species and are consistent with the expected *fac*-PtC_3 geometry, and the criterion that a MePt group *trans* to halide gives ^2J(PtH) > 70 Hz whereas a MePt group *trans* to imine gives ^2J(PtH) < 70 Hz is most useful in structure assignments.[3,5,10,11] The iminic proton resonances were present at δ 8.51 with ^3J(PtH) = 50 Hz and at δ 8.82 with ^3J(PtH) = 36 Hz, thus establishing that both imine groups remain coordinated to the platinum(II) center. A second set of methylplatinum and imine resonances indicated the presence of a second, minor stereoisomer, which was assigned structure **6b** (or **6d**) (Chart 1). The ^{1}H NMR data are similar to those for **6a** (Table 1), and so a similar *fac*-PtC_3 structure is established. Integration of the methylplatinum and imine ^{1}H NMR signals of the mixture gave the diastereomeric ratio (**6a** + **6c**):(**6b** + **6d**) = 2.3, establishing a significant degree of stereoselectivity during the intermolecular oxidative addition of iodomethane to complex **4**. The absolute configuration of the major stereoisomer **6a**,**c** was assigned as *R*,*R*-*C* (*S*,*S*-*A*) on the basis of X-ray structural data obtained from the analogous products from reaction of **4** with iodoethane and benzyl bromide (see below) and the similarity of ^{1}H NMR data between these complexes (Table 1). The absolute configuration of the minor diastereomer, **6b**,**d** could then be assigned as *R*,*R*-*A* (*S*,*S*-*C*).

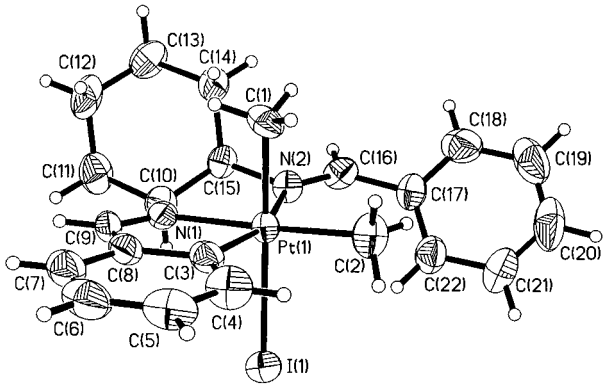

Figure 2. View of the structure of the *S*,*R*-*A* enantiomer of complex **7a**.

Racemic [PtMe{*cis*-1-(N=CHC_6H_4)-2-(N=CHC_6H_5)-C_6H_{10}}] (**5**) reacted similarly with iodomethane to give largely one diastereomer of [$PtIMe_2${*cis*-1-(N=CHC_6H_4)-2-(N=CHC_6H_5)C_6H_{10}}] (**7**), shown to have structure **7a** (or **7c**). Minor resonances were observed due to one or more minor species, but the low abundance of about 5%, coupled with partial overlap of key resonances with the much stronger resonances of **7a**, did not allow structural assignment. NMR data for **7a** are given in Table 1 and are fully consistent with the proposed structure. The stereochemistry of the major isomer **7a** was established as *S*,*R*-*A* (*R*,*S*-*C*) by an X-ray structure determination. A view of the structure of the *S*,*R*-*A* enantiomer is shown in Figure 2, and selected bond lengths and angles are provided in Table 3. The structure confirms the presence of an octahedrally coordinated platinum(IV) center, with a *fac*-PtC_3 geometry for the carbon donor ligands, with the absolute configuration of the complex being *S*,*R*-*A* (*R*,*S*-*C*). The tridentate N,N,C ligand adopts the expected meridional coordination, and the geometry around platinum(IV) is distorted from octahedral due to the constraints of this ligand. The Pt-*C* bond lengths are normal, and the Pt(1)−I(1) bond length of 2.7844(9) Å is also within the expected range.[15] With respect to the platinum−imine bonds, the distance N(2)−Pt of 2.216(8) Å is significantly longer than the N(1)−Pt distance of 2.075(7) Å, though both are *trans* to carbon donors; this could be due to steric interactions between the nonmetalated phenylimine fragment and the crowded equatorial site occupied by the C2 methyl ligand. Figure 2 shows that, for the major isomer **7a**, the iodide ligand is *anti* to the cyclohexane ring, which lies above the plane containing the N,N,C tridentate ligand, while the methyl group is in a position *syn* to the cyclohexyl group. This stereochemistry is perhaps expected for the product of thermodynamic control, since

(14) Crespo, M. *Polyhedron* **1996**, *15*, 1981.

(15) Levy, C. J.; Vittal, J. J.; Puddephatt, R. J. *Organometallics* **1996**, *15*, 2108 and references therein.

Downloaded by CARLI CONSORTIUM on June 30, 2009
Published on May 23, 1998 on http://pubs.acs.org | doi: 10.1021/om980065z

Table 3. Selected Bond Distances and Angles for Complex 7a[a]

(a) Bond Lengths (Å)

Pt(1)−C(3)	2.00(1)	Pt(1)−C(1)	2.07(1)
Pt(1)−C(2)	2.07(1)	Pt(1)−N(1)	2.075(7)
Pt(1)−N(2)	2.216(8)	Pt(1)−I(1)	2.7844(9)
N(1)−C(9)	1.28(1)	N(1)−C(10)	1.48(1)
N(2)−C(16)	1.28(1)	N(2)−C(15)	1.53(1)
C(3)−C(8)	1.43(1)	C(8)−C(9)	1.43(2)
C(10)−C(15)	1.51(1)	C(16)−C(17)	1.46(1)

(b) Bond Angles (deg)

C(3)−Pt(1)−C(1)	84.9(4)	C(3)−Pt(1)−C(2)	94.3(4)
C(1)−Pt(1)−C(2)	83.8(5)	C(3)−Pt(1)−N(1)	81.6(4)
C(1)−Pt(1)−N(1)	92.6(4)	C(2)−Pt(1)−N(1)	174.8(4)
C(3)−Pt(1)−N(2)	160.2(3)	C(1)−Pt(1)−N(2)	92.2(4)
C(2)−Pt(1)−N(2)	104.9(4)	N(1)−Pt(1)−N(2)	78.9(3)
C(3)−Pt(1)−I(1)	90.6(3)	C(1)−Pt(1)−I(1)	175.2(3)
C(2)−Pt(1)−I(1)	94.8(3)	N(1)−Pt(1)−I(1)	88.5(2)
N(2)−Pt(1)−I(1)	92.6(2)	C(9)−N(1)−C(10)	129.0(8)
C(9)−N(1)−Pt(1)	114.0(7)	C(10)−N(1)−Pt(1)	116.6(6)
C(16)−N(2)−C(15)	113.7(8)	C(8)−C(3)−Pt(1)	110.6(7)
C(3)−C(8)−C(9)	116.9(9)	N(1)−C(9)−C(8)	116.7(9)
N(2)−C(16)−C(17)	127.1(9)		

[a] Symmetry transformations used to generate equivalent atoms: #1 $-x, -y + 1, -z$.

Downloaded by CARLI CONSORTIUM on June 30, 2009
Published on May 23, 1998 on http://pubs.acs.org | doi: 10.1021/om980065z

it may minimize steric effects. However, it is not easily explained if the structure represents the product of kinetic control since, in an S_N2 mechanism leading to *trans* oxidative addition, the methyl group should approach the least hindered face, leading ultimately to **7b**. Of course, at this stage it was not possible to determine if *trans* or *cis* oxidative addition had occurred since structures **7a**,**c** and **7b**,**d** are equivalent. To gain further insight into the puzzling observations, it was decided to monitor the reaction of **5** with CD_3I by ^1H NMR spectroscopy.

Reactions with CD_3I. The reaction of racemic [PtMe{*cis*-1-(N=CHC_6H_4)-2-(N=CHC_6H_5)C_6H_{10}}] (**5**) with CD_3I was followed by ^1H NMR spectroscopy at ambient temperature in CD_2Cl_2 solution (Figure 3a). The reaction product gave a major methylplatinum(IV) resonance at δ 0.82 with ^2J(PtH) = 72 Hz, identical with the MePt resonance *trans* to iodide in **7a** (or **7c**) (Table 1), which is therefore assigned to **7c***. There was also a minor resonance at δ 0.87 with ^2J(PtH) = 66 Hz, which could be due to the MePt group *trans* to N in either **7a*** or **7b*** (the resonances are accidentally degenerate) but will be shown to be due to **7b***. Hence, the product is identified as largely **7c***, which is formed by overall *cis* oxidative addition of CD_3I to platinum(II), a process for which there are few precedents and which is not understood in mechanistic terms.[2] The product **7b***, formed by *trans* oxidative addition, was also present, but in low abundance. The ratio **7c***:**7b*** = 9.

When the analogous reaction with CD_3I was carried out with racemic [PtMe{*trans*-1-(N=CHC_6H_4)-2-(N=CH-C_6H_5)C_6H_{10}}] (**4**), the major product could be identified by ^1H NMR as **6a*** (Chart 1, Figure 3b) which is formed largely by *trans* oxidative addition of CD_3I. Thus, the most intense resonance appeared at δ 0.78 with ^2J(PtH) = 67 Hz, indicating that the CH_3 group is *trans* to imine in an equatorial position in **6a***, while there was only a minor resonance at δ 0.67 with ^2J(PtH) = 71 Hz due to the axial methyl group in **6c***. The ratio **6a***:**6c*** = 2.8. However, the minor diastereomer is identified as largely **6d***, which is formed by *cis* oxidative addition of CD_3I. Thus, the major MePt resonance occurred at δ 0.66 with ^2J(PtH) = 72 Hz, placing the CH_3 ligand in an axial position *trans* to iodide, with only a minor MePt resonance at δ 0.95 with ^2J(PtH) = 66 Hz due to the MePt group *trans* to imine in **6b*** (Figure 3b). The ratio **6d***:**6b*** = 2.8. In addition, the ratios **6a***:**6d*** = **6c***:**6b*** = 2.3.

The stereochemical assignments discussed above were unexpected, and so it was considered necessary to confirm the ^1H NMR assignments on which they are based. This was accomplished by use of nuclear Overhauser effect (NOE) difference spectroscopy (Chart 3).[16] The NOE difference spectra for the platinum(II) complex [PtMe{*cis*-1-(N=CHC_6H_4)-2-(N=CHC_6H_5)C_6H_{10}}] (**5**) demonstrated a significant enhancement between the ortho H_a protons of the phenylimine group and the methylplatinum H_b protons (1.9% enhancement), consistent with the close proximity of the H_a and H_b protons (Chart 3) expected by analogy with the X-ray structure of the related complex **4** shown in Figure 1. The X-ray structure of **7a** (Figure 2) shows that a corresponding ortho hydrogen atom of the phenylimino group lies closer to the equatorial (H_b) than to the axial (H_c) methylplatinum group and so the NOE difference spectra should give an independent assignment for these two resonances. The results are shown in Chart 3 (in which the positions of H_b and H_c are based on the original assignments discussed earlier), and they confirm the original assignments since there is a larger NOE associated with the methylplatinum resonance assigned to be in the equatorial position. Similarly, there was a greater NOE effect between the phenyl proton H_a of the imine group and the equatorial over the axial methyl group in **6a** (Chart 3). The conclusions reached on the stereochemistry of the oxidative addition of CD_3I are therefore validated.

Reaction of [PtMe{*cis*-1-(N=CHC_6H_4)-2-(N=CH-C_6H_5)C_6H_{10}}] (5) with CD_3I at Low Temperature. Since the primary step in the S_N2 mechanism of oxidative addition of alkyl halides must place the alkyl group in an axial position,[3] it was surprising that the major product of oxidative addition of CD_3I to **5**, namely **7c***, contained the CD_3 group in the equatorial position. Low-temperature NMR studies of the oxidative addition of MeI and CD_3I with **5** were therefore carried out to determine if **7c*** was really the first-formed product.

MeI or CD_3I was added to a solution of complex **5** in CD_2Cl_2 at −78 °C, and the progress of the reaction was followed by ^1H NMR spectroscopy; spectra for the reaction with CD_3I are shown in Figure 4. Reaction began to occur at −60 °C, and the first-formed product with MeI was determined to be **7b** (**7d**). The experiment with CD_3I distinguishes between these complexes and showed that **7b*** was the kinetic product. As the solution was warmed, peaks due to **7b*** decayed and those due to **7c*** grew. The apparent isomerization reaction of **7b*** to **7c*** was only slightly slower than the oxidative addition and both appeared to be complete at −20 °C, an equilibrium between **7b*** and **7c*** being present at room temperature.

In a similar low-temperature study of the reaction of CD_3I with **4**, the initial products at −60 °C were mostly

(16) Derome, A. E. *Modern NMR Techniques for Chemistry Research*; Pergamon Press: New York, 1987; Chapter 5.

Downloaded by CARLI CONSORTIUM on June 30, 2009
Published on May 23, 1998 on http://pubs.acs.org | doi: 10.1021/om980065z

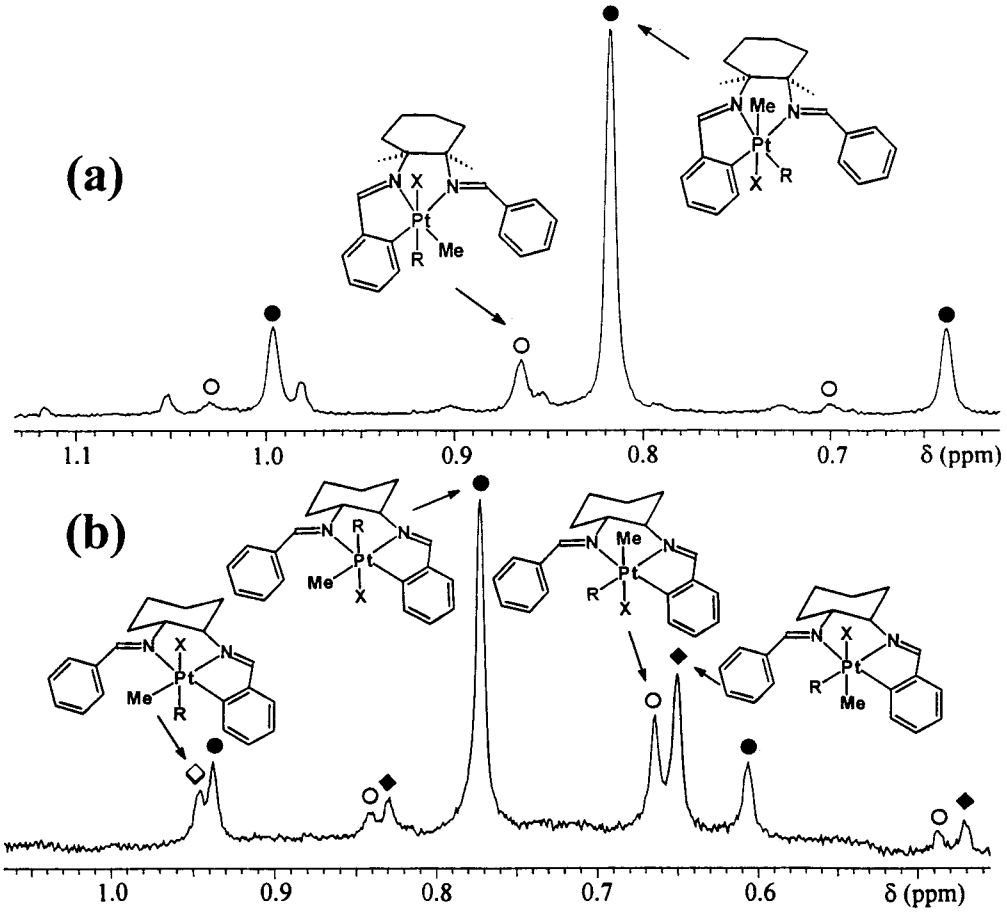

Figure 3. ^{1}H NMR spectra (200 MHz) in the MePt region of the products of reaction of CD_3I with (a) complex **5** (the major resonance is due to **7c*** and the minor one to **7b***) and (b) complex **4** (peaks centered at δ 0.95, 0.78, 0.67, and 0.66 are due to **6b***, **6a***, **6c***, and **6d***, respectively).

Chart 3

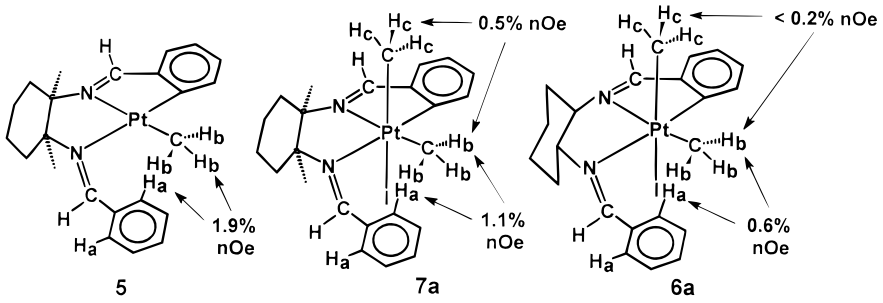

6a* and **6b***, with **6a***/**6b*** = ca. 4, only minor amounts of **6c*** and **6d*** being present at the stage when no starting complex **4** remained. As the reaction mixture was warmed, the products **6c*** and **6d*** grew in and the final product ratio was close to that observed in the room-temperature reaction. Thus, it seems that **6a*** and **6b*** are the primary products and that **6c*** and **6d*** are formed subsequently by isomerization of the primary products.

Oxidative Addition of Ethyl Iodide. Reaction of **4** with iodoethane in THF was slower than with iodomethane, requiring approximately 4 h at ambient temperature to reach completion. The product was shown by ^{1}H NMR spectroscopy to be a single stereoisomer of [PtIMeEt{*trans*-1-(N=CHC_6H_4)-2-(N=CHC_6H_5)C_6H_{10}}] (**8a**, ca.100% diastereoselectivity; Chart 1). The ^{1}H NMR data (Table 1) are consistent with *fac*-PtC_3 geometry and *trans* oxidative addition of the Et−I bond, fixing the methyl group in an equatorial position *trans* to an imine ligand and the ethylplatinum group in an axial position *trans* to iodide. However, the NMR data cannot distinguish between the possible structures **8a** and **8b**. The progress of the reaction in CD_2Cl_2 solution at room temperature was monitored by ^{1}H NMR spectroscopy, and it was shown that there were no long-lived intermediates en route to the observed product and that no subsequent isomerization occurred over several days.

The complex was fully characterized as **8a** by an X-ray structure determination. A view of the structure of the enantiomer (*R*,*R*-*C*)-[PtIMeEt{*trans*-1-(N=CHC_6H_4)-2-(N=CHC_6H_5)C_6H_{10}}] is shown in Figure 5, and selected bond lengths and angles are provided in Table 4. The structure confirms the structural deductions based on

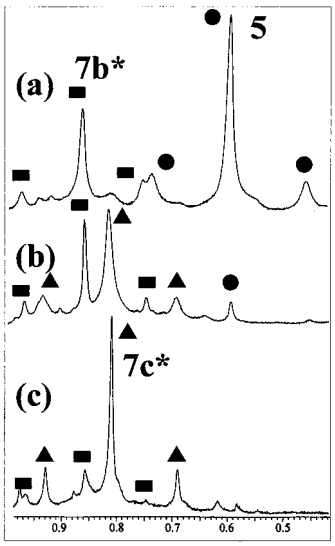

Figure 4. ^{1}H NMR spectra (300 MHz) of the products of reaction of CD_3I with complex **5**: (a) at −50 °C, **5** and **7b*** present; (b) at −30 °C, **5** (trace), **7b***, and **7c*** present; (c) at 20 °C, **7b*** (minor) and **7c*** (major) present.

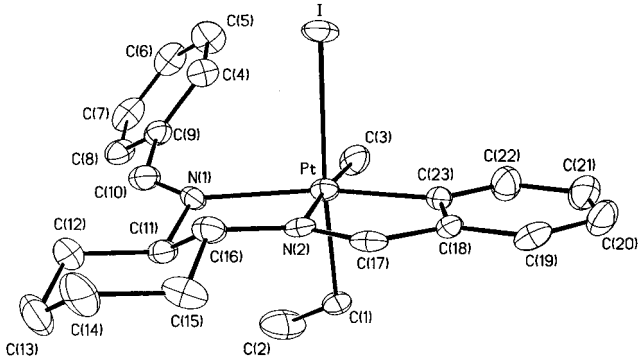

Figure 5. View of the structure of the *R,R*−*C* enantiomer of complex **8a**.

Table 4. Selected Bond Distances and Angles for Complex 8a

(a) Bond Lengths (Å)

Pt−C(23)	2.00(1)	Pt−N(2)	2.057(8)
Pt−C(3)	2.05(1)	Pt−C(1)	2.120(9)
Pt−N(1)	2.217(9)	Pt−I	2.8042(7)
N(1)−C(10)	1.27(1)	N(1)−C(11)	1.52(1)
N(2)−C(17)	1.29(1)	N(2)−C(16)	1.45(1)
C(1)−C(2)	1.48(2)	C(9)−C(10)	1.47(2)
C(11)−C(16)	1.52(2)	C(17)−C(18)	1.45(1)
C(18)−C(23)	1.42(1)		

(b) Bond Angles (deg)

C(23)−Pt−N(2)	82.0(4)	C(23)−Pt−C(3)	93.6(5)
N(2)−Pt−C(3)	175.3(4)	C(23)−Pt−C(1)	86.1(4)
N(2)−Pt−C(1)	91.9(4)	C(3)−Pt−C(1)	86.3(5)
C(23)−Pt−N(1)	160.8(4)	N(2)−Pt−N(1)	79.0(4)
C(3)−Pt−N(1)	105.3(4)	C(1)−Pt−N(1)	92.0(3)
C(23)−Pt−I	88.8(3)	N(2)−Pt−I	86.0(2)
C(3)−Pt−I	95.5(4)	C(1)−Pt−I	174.8(3)
N(1)−Pt−I	92.2(2)	C(10)−N(1)−C(11)	118.0(9)
C(10)−N(1)−Pt	135.2(8)	C(11)−N(1)−Pt	106.4(6)
C(17)−N(2)−C(16)	128.9(9)	C(17)−N(2)−Pt	113.7(7)
C(16)−N(2)−Pt	117.2(7)	C(2)−C(1)−Pt	116.3(7)
N(1)−C(10)−C(9)	129.0(11)	N(2)−C(16)−C(11)	107.6(9)
N(2)−C(17)−C(18)	117.6(9)	C(18)−C(23)−Pt	111.5(8)

NMR evidence and also defines the chirality at platinum, in particular that the ethyl group is *syn* to the cyclohexyl group which, in the ligand based on *trans*-diaminocyclohexane, appears to create less steric hindrance at this site than in complex **7a**, in which the ligand is based on *cis*-diaminocyclohexane. As in **7a**, meridional coordination is adopted by the N,N,C tridentate ligand. The Pt−N(1) distance of 2.22(1) Å is long, and this may indicate steric effects between the uncyclometalated phenylimine fragment and the adjacent iodide and $C(3)H_3$ groups; the greater bond distortion from the ideal 90° is N(1)−Pt−C(3) = 105.3(4)°, indicating that the greatest steric congestion may be in the equatorial plane. Clearly then, a structure with the ethyl group in the equatorial plane would not be favored. If this analysis is correct, then it is not surprising that the ethyl iodide attacks the face *syn* to the cyclohexyl group and that it remains in the axial site; that is, **8a** is favored by both kinetic and thermodynamic factors.

The reaction of [PtMe{*cis*-1-(N=CHC_6H_4)-2-(N=CHC_6H_5)C_6H_{10}}] (**5**) with iodoethane in THF gave [PtIMeEt{*cis*-1-(N=CHC_6H_4)-2-(N=CHC_6H_5)C_6H_{10}}] (**9b**) with essentially complete stereoselectivity (Chart 2). Monitoring by NMR again indicated that no long-lived intermediates were formed, and **9b** could be isolated in analytically pure form. However, during the attempted growth of single crystals of **9b**, subsequent slow hydrolysis of the nonmetalated imine group occurred to give [PtIMeEt{*cis*-1-(N=CHC_6H_4)-2-(NH_2)C_6H_{10}}] (**10**) (eq 2).

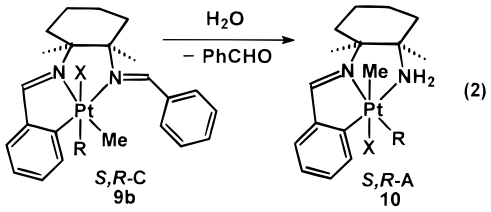

In the ^{1}H NMR spectrum of **9b** (Table 1), the methylplatinum resonance occurred at δ 0.87 with ^3J(PtH) = 67 Hz, indicating that the methyl group remains in the equatorial site in the platinum(IV) product and hence that *trans* oxidative addition occurs selectively. The two imine proton resonances at δ 8.51 and 8.85 each showed well-resolved ^{195}Pt satellites, confirming that both imine groups were still present and were coordinated to platinum. The data do not define the chirality at platinum and so do not distinguish between structures **9a** and **9b**, and so the assignment as **9b** is based on other evidence discussed below.

The hydrolysis of **9b** to give **10** (along with unidentified complexes which could be isomers of **10**) could be monitored by ^{1}H NMR in CD_2Cl_2 on the basis of the growth of the aldehyde resonance of PhCHO at δ 10.0. In contrast to **9b**, the ^{1}H NMR spectrum of **10** (Table 1) contained a methylplatinum resonance at δ 0.93 with ^2J(PtH) = 72 Hz, indicating that the methyl group was *trans* to iodide in **10**. Hence, complex **10** was also characterized by an X-ray structure determination. A view of the structure of the *S,R-A* enantiomer is shown in Figure 6, and selected bond lengths and angles are in Table 5. The complex contains an octahedral platinum(IV) center with a meridional tridentate *cis*-1-(N=CHC_6H_4)-2-(NH_2)C_6H_{10} ligand. As deduced by NMR, the methyl group is *trans* to iodide and the ethyl group lies in the equatorial plane, corresponding to a product of overall *cis* oxidative addition of ethyl iodide. As in **7a**, the other platinum(IV) complex with a tridentate ligand derived from *cis*-diaminocyclohexane, the rela-

Downloaded by CARLI CONSORTIUM on June 30, 2009
Published on May 23, 1998 on http://pubs.acs.org | doi: 10.1021/om980065z

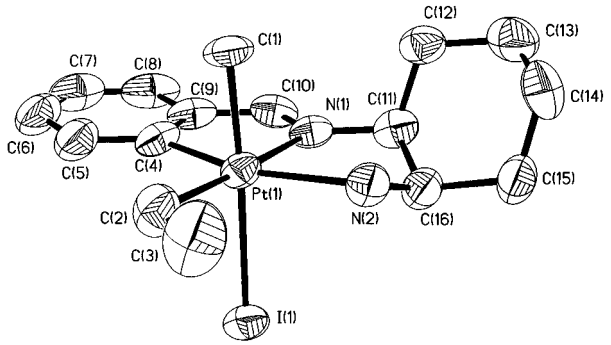

Figure 6. View of the structure of the *S,R-A* enantiomer of complex **10**.

Table 5. Selected Bond Distances and Angles for Complex 10

(a) Bond Lengths (Å)

Pt(1)−C(4)	2.009(8)	Pt(1)−C(1)	2.067(7)
Pt(1)−N(1)	2.069(7)	Pt(1)−C(2)	2.076(8)
Pt(1)−N(2)	2.193(6)	Pt(1)−I(1)	2.7865(7)
N(1)−C(10)	1.27(1)	N(1)−C(11)	1.46(1)
N(2)−C(16)	1.51(1)	C(2)−C(3)	1.44(1)
C(4)−C(9)	1.39(1)	C(9)−C(10)	1.47(1)
C(11)−C(16)	1.52(1)		

(b) Bond Angles (deg)

C(4)−Pt(1)−C(1)	86.6(3)	C(4)−Pt(1)−N(1)	80.8(3)
C(1)−Pt(1)−N(1)	92.5(3)	C(4)−Pt(1)−C(2)	97.0(4)
C(1)−Pt(1)−C(2)	86.4(4)	N(1)−Pt(1)−C(2)	177.6(3)
C(4)−Pt(1)−N(2)	159.1(3)	C(1)−Pt(1)−N(2)	91.4(3)
N(1)−Pt(1)−N(2)	78.5(2)	C(2)−Pt(1)−N(2)	103.6(3)
C(4)−Pt(1)−I(1)	92.7(2)	C(1)−Pt(1)−I(1)	175.7(3)
N(1)−Pt(1)−I(1)	91.5(2)	C(2)−Pt(1)−I(1)	89.6(3)
N(2)−Pt(1)−I(1)	90.8(2)	C(10)−N(1)−C(11)	126.2(7)
C(10)−N(1)−Pt(1)	115.2(6)	C(11)−N(1)−Pt(1)	118.6(5)
C(16)−N(2)−Pt(1)	107.8(5)	C(3)−C(2)−Pt(1)	116.7(7)
C(9)−C(4)−Pt(1)	111.7(6)	C(4)−C(9)−C(10)	116.7(7)
N(1)−C(10)−C(9)	115.6(8)	N(1)−C(11)−C(16)	107.5(7)
N(2)−C(16)−C(11)	110.4(6)		

tively smaller methyl and larger iodide groups lie *syn* and *anti* to the bulky cyclohexyl group, respectively. The absence of a free PhCH=N group in **10** leads to lower steric hindrance in the equatorial site where the ethyl group is found. Thus, **10** is expected to be the most thermodynamically stable of the possible isomers.

Oxidative Addition of *n*-Propyl Iodide. The oxidative addition of propyl iodide to [PtMe{*trans*-1-(N=CHC_6H_4)-2-(N=CHC_6H_5)C_6H_{10}}] (**4**) required several hours to reach completion at ambient temperature, and some product decomposition occurred during this period. Nevertheless, it was clear that a single diastereomer of [PtIMe(*n*-Pr){*trans*-1-(N=CHC_6H_4)-2-(N=CHC_6H_5)C_6H_{10}}] (**11**) was formed and the structure was readily assigned as **11a** (Chart 1), based on the similarity of the ^{1}H NMR data (Table 1) to those of the structurally characterized complex **8a**.

The reaction of propyl iodide with **5** was also slow and gave a single diastereomer of [PtIMe(*n*-Pr){*cis*-1-(N=CHC_6H_4)-2-(N=CHC_6H_5)C_6H_{10}}] (**12**), which was easily separated from minor decomposition products by recrystallization. A comparison of the ^{1}H NMR data of complex **12** with those of **9** indicates that these compounds are isostructural and the *S,R-C* (or *R,S-A*) structure **12b** is tentatively proposed.

Oxidative Addition of Benzyl Bromide. Complexes **4** and **5** each reacted rapidly with benzyl bromide in THF solution at room temperature, and the stereoselectivities achieved in these reactions closely resembled those observed for the similarly rapid reactions with methyl iodide. Thus, complex **4** gave two diastereomers of [PtBrMeBz{*trans*-1-(N=CHC_6H_4)-2-(N=CH-C_6H_5)C_6H_{10}}] (**13**) on reaction with benzyl bromide, as shown by the ^{1}H NMR spectra. The ^{1}H NMR spectra (Table 1) define the structures as **13a** and **13b**, and the major isomer was characterized as **13a** by an X-ray structure determination. The methylplatinum protons were represented by signals at δ 0.86 with ^3J(PtH) = 66 Hz for **13a** and δ 1.01 with ^3J(PtH) = 66 Hz for **13b**, and the coupling constants confirm that the MePt groups are *trans* to imine in both cases. The ratio of isomers **13a**:**13b** = 6:1 was determined by integration of methylplatinum and imine resonances. The benzylic protons in **13a** and **13b** are expected to be diastereotopic; the resonances for these protons were well-resolved for the major isomer only and appeared as two doublets at δ 2.66 and 2.87 with coupling constants ^2J(PtH) = 93 and 102 Hz, respectively. These large ^2J(PtH) coupling constants are typical of benzylplatinum(IV) complexes.[17] The imine resonances for both stereoisomers showed well-resolved platinum satellites, which confirms the N,N,C tridentate ligand coordination.

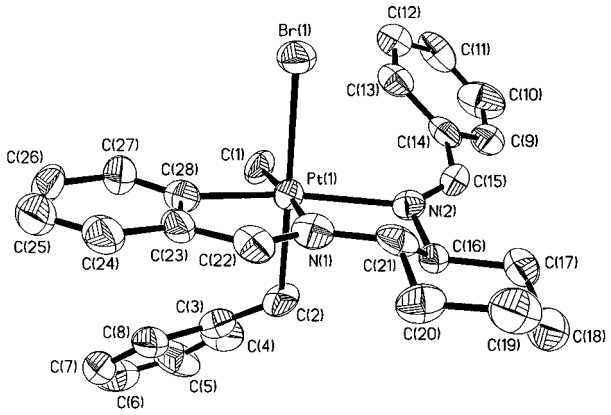

Figure 7. View of the structure of the *S,S-A* enantiomer of complex **13a**.

Single crystals of isomer **13a** grew preferentially from a mixture of diastereomers **13a** and **13b** (confirmed by NMR of the single crystals). A view of the structure of the *S,S-A* enantiomer of **13a** is provided in Figure 7, and selected bond lengths and angles are given in Table 6. The platinum atom is octahedrally coordinated by the N,N,C tridentate ligand and monodentate bromide, methyl, and benzyl ligands. The usual *fac*-PtC_3 geometry, with *mer*-N,N,C coordination of the tridentate ligand, is present. The nonmetalated phenylimine is *syn* to the bromide ligand and *anti* to the benzyl fragment. The N(2)−Pt distance of 2.24(1) Å is long and, as for related complexes, this may be partly attributed to steric hindrance between the phenyl substituent and equatorial methyl and axial bromide groups. The benzyl ligand bends under and toward the cyclometalated ring to minimize steric effects, but there is no evidence for significant π-stacking effects between the aromatic groups.

Complex **5** gave a single stereoisomer of [PtIMe(Bz)-{*cis*-1-(N=CHC_6H_4)-2-(N=CHC_6H_5)C_6H_{10}}] (**14**, ca. 100%

(17) Rendina, L. M.; Vittal, J. J.; Puddephatt, R. J. *Organometallics* **1995**, *14*, 2188.

Downloaded by CARLI CONSORTIUM on June 30, 2009
Published on May 23, 1998 on http://pubs.acs.org | doi: 10.1021/om980065z

Table 6. Selected Bond Distances and Angles for Complex 13a

(a) Bond Lengths (Å)			
Pt(1)−C(28)	2.01(1)	Pt(1)−N(1)	2.06(1)
Pt(1)−C(1)	2.09(1)	Pt(1)−C(2)	2.117(8)
Pt(1)−N(2)	2.24(1)	Pt(1)−Br(1)	2.605(1)
N(1)−C(22)	1.26(2)	N(1)−C(21)	1.47(2)
N(2)−C(15)	1.25(2)	N(2)−C(16)	1.49(2)
C(2)−C(3)	1.47(2)	C(14)−C(15)	1.47(2)
C(16)−C(21)	1.53(2)	C(22)−C(23)	1.47(2)
C(23)−C(28)	1.44(2)		
(b) Bond Angles (deg)			
C(28)−Pt(1)−N(1)	82.3(5)	C(28)−Pt(1)−C(1)	94.0(5)
N(1)−Pt(1)−C(1)	175.1(4)	C(28)−Pt(1)−C(2)	91.7(7)
N(1)−Pt(1)−C(2)	90.4(4)	C(1)−Pt(1)−C(2)	86.5(4)
C(28)−Pt(1)−N(2)	162.8(4)	N(1)−Pt(1)−N(2)	80.5(4)
C(1)−Pt(1)−N(2)	103.1(4)	C(2)−Pt(1)−N(2)	87.6(6)
C(28)−Pt(1)−Br(1)	86.9(3)	N(1)−Pt(1)−Br(1)	86.9(3)
C(1)−Pt(1)−Br(1)	96.1(3)	C(2)−Pt(1)−Br(1)	177.0(4)
N(2)−Pt(1)−Br(1)	93.0(2)	C(22)−N(1)−Pt(1)	117(1)
C(21)−N(1)−Pt(1)	115.1(7)	C(16)−N(2)−Pt(1)	104.4(8)
C(3)−C(2)−Pt(1)	121.1(9)	N(2)−C(15)−C(14)	130(1)
N(2)−C(16)−C(21)	110(1)	N(1)−C(21)−C(16)	108.4(9)
N(1)−C(22)−C(23)	113(2)	C(28)−C(23)−C(22)	120(1)
C(23)−C(28)−Pt(1)	108(1)		

Table 7. Molecular Mechanics Calculations of Relative Energies (kcal/mol) of Isomers a−d[a]

complex, R, X	a	b	c	d
		trans Isomers		
6, Me, I	32.92	32.91	32.92	32.91
8, Et, I	34.76	34.78	36.53	36.83
11, Pr, I	34.09	34.10	35.51	35.98
13, Bz, Br	24.98	24.81	30.70	31.38
		cis Isomers		
7, Me, I	29.92	30.29	29.92	30.29
9, Et, I	31.93	32.26	33.95	33.94
12, Pr, I	31.09	31.58	32.86	32.97
14, Bz, Br	22.01	22.17	27.88	27.16

[a] For structures of isomers, see Charts 1 and 2.

stereoselectivity) on reaction with benzyl bromide. The ^{1}H NMR data show that the methyl group is equatorial and so define the structure as **14a** or **14b**; the structure **14b** is tentatively proposed on the basis of the data discussed below.

Molecular Mechanics Calculations.[18] To provide additional insight into the thermodynamic and kinetic factors involved in the stereoselectivity of the oxidative-addition reactions, molecular mechanics calculations were carried out for each of the complexes in Charts 1 and 2 and the calculated energies are listed in Table 7. For the cases with R = Et, Pr, or Bz, energies were calculated for several conformations formed by rotation about the Pt-*C* bond and the lowest energy found is reported.

Note that when R = Et, Pr, or Bz, the energies of isomers **c** and **d** (R equatorial) are always significantly higher than those of isomers **a** and **b** (R axial), and this is clearly due to strong steric effects between the alkyl group R in the equatorial site and the phenyl substituent of the nonmetalated imine. Figure 8 shows space-filling diagrams for isomers of **9** with the ethyl group axial or equatorial to illustrate this effect. As found experimentally, this site is expected to be occupied by the smallest alkyl group, namely the methyl group in the thermodynamically favored isomers. The energy differences of 1.4−5.0 kcal/mol would not preclude formation of compounds with equatorial groups R as transient intermediates or transition states in potential isomerization processes.

(18) CACHE Scientific Inc., Version 3.7, 1992.

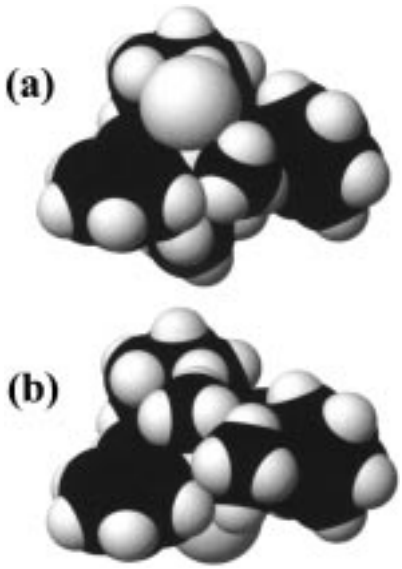

Figure 8. Space-filling models of complexes (a) **9b** and (b) **9c** in orientations similar to those in Chart 2. Complex **9c** is not favored, due to steric congestion at the ethyl group in the equatorial position.

The calculations predict much smaller energy differences between the isomers **a** and **b**, in most cases probably within the error limits of the calculations. Thus, for compounds based on *trans*-diaminocyclohexane, isomer **b** is favored for **6** and **13** but isomer **a** for **8** and **11**. For compounds based on *cis*-diaminocyclohexane, isomer **a** is preferred in all cases. This similarity is not surprising, since the groups R and X are expected to have similar steric bulk (rotation about the Pt-*C* bond allows R to adopt a favored conformation). Clearly then, the stereoselectivity in oxidative addition cannot be understood in terms of the thermodynamic stability of the products but must be addressed in terms of the transition state for the first step in the oxidative addition reaction, that is in terms of the relative steric hindrance to approach of R−X to either face of the platinum(II) reagent, coupled with consideration of possible isomerization processes.

For complex **10**, in which the nonmetalated phenyl group is no longer present, the structures with an equatorial ethyl group are calculated to be more stable than those with an axial ethyl group by 1.9 kcal/mol, the opposite trend from that for **9**. Hence, the isomerization from axial to equatorial ethyl on hydrolysis of **9** to **10** is favored thermodynamically. Since the structure of **10** is established, this isomerization provides strong support for the suggestion that **9** is formed in the isomeric form **9b**, even though the molecular mechanics calculations indicate that **9a** should be preferred slightly on thermodynamic grounds.

Discussion

Diastereoselective Oxidative Addition of MeI and CD_3I. The reaction of complex **5** with MeI or CD_3I to give **7** occurs with >90% stereoselectivity, and the mechanism shown in Scheme 3 can be deduced from

Downloaded by CARLI CONSORTIUM on June 30, 2009
Published on May 23, 1998 on http://pubs.acs.org | doi: 10.1021/om980065z

Downloaded by CARLI CONSORTIUM on June 30, 2009
Published on May 23, 1998 on http://pubs.acs.org | doi: 10.1021/om980065z

Scheme 3

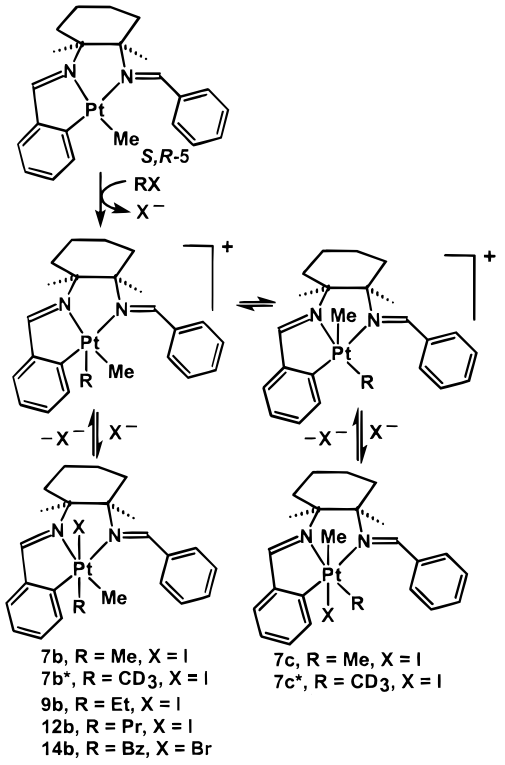

low-temperature NMR studies. In complex **5** steric hindrance by the cyclohexyl group above the plane (as drawn in Scheme 3) is greater than steric hindrance below the plane arising from the free phenyl substituent of the imine, therefore, attack of methyl iodide occurs below the plane only, as shown in Scheme 3. The primary product observed at low temperature is thus **7b** or **7b***. The ionic intermediates cannot be detected, since they are short-lived in CD_2Cl_2 solvent.[3] As expected in an S_N2 mechanism,[3] and proved in the case of **7b***, the kinetic product is formed by *trans* oxidative addition. When the temperature is raised, resonances due to **7b** or **7b*** decay and those due to **7c** or **7c*** grow and equilibrium between **7b** and **7c** is reached below room temperature. Complex **7c*** appears to be formed by *cis* oxidative addition, but this is clearly deceptive. The platinum(IV) complexes are stable to reductive elimination, and **7c*** arises by isomerization of **7b*** within the platinum(IV) system. Thus, loss of iodide gives the cationic intermediate, which can undergo methyl migration between filled and empty sites, *but only in the meridional plane not occupied by the tridentate ligand*. A concerted migration of both methyl groups is likely to avoid the unfavorable situation in which two methyl groups are mutually *trans*. There are two chief differences between the chemistry of **5** and that of the simpler complexes such as [$PtMe_2$(2,2′-bipyridine)]. First, the present system gives much easier equilibration between isomers; this is attributed to much easier iodide dissociation leading to the five-coordinate intermediate with the bulkier ligand in **5**. Second, the presence of the *mer*-tridentate ligand in **5** restricts the migration to a linear process in the other meridional plane and does not allow a turnstile rotation process which would lead to scrambling between all possible isomers. It is this feature that leads to a particularly clear picture of the oxidative-addition and isomerization mechanisms as depicted in Scheme 3.

Scheme 4

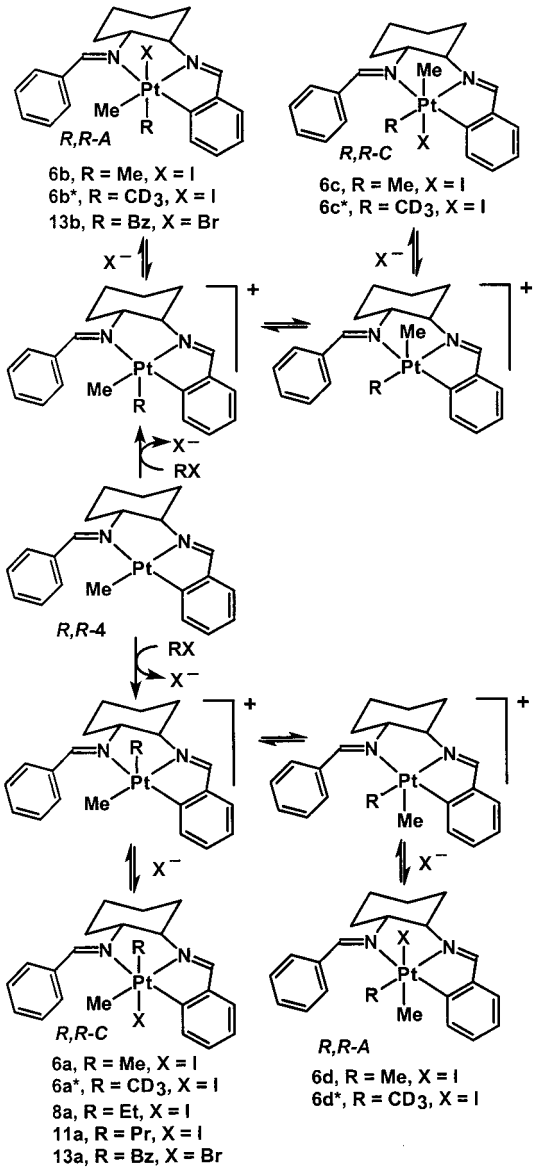

The oxidative addition of CD_3I to **4** gives all four possible isomers of the product of oxidative addition **6***, therefore, the interpretation is somewhat complex (Scheme 4). The major product of oxidative addition of MeI to **4** is assigned structure **6a**,**c** on the basis of the similarity of its NMR data (Table 1) to those of the structurally characterized complex **8a** and **13a**, the minor product being **6b**,**d** (Chart 1). Use of CD_3I in place of MeI then distinguishes between equivalent pairs of complexes, and the major product is shown to be **6a***, formed by *trans* oxidative addition, rather than **6c***. Similarly, the minor isomer is shown to be **6d***, formed by overall *cis* oxidative addition, rather than **6b***. These data are fully consistent with the mechanism of Scheme 4. Thus, the ratio of products (**6a*** + **6d***)/(**6b*** + **6c***) = 2.8 is determined by the stereoselectivity of the primary step in the oxidative addition, whereas the ratio K = **6a***/**6d*** = **6c***/**6b*** = 2.3 is determined by the equilibrium constant between these pairs of complexes. The primary reaction at −60 °C gives **6a*** and **6b***, and the initial ratio **6a***/**6b*** is also

Downloaded by CARLI CONSORTIUM on June 30, 2009
Published on May 23, 1998 on http://pubs.acs.org | doi: 10.1021/om980065z

expected to be 2.8. The observed value of **6a*/6b*** = 4 is higher, but this is attributed to partial isomerization of **6b*** even at −60 °C; the ratio **6a*/6b*** increased with time to a final value of 5.7, very similar to the value obtained in the room-temperature reaction. Since there is rather little difference in steric effects above and below the plane, the energy differences between the isomers of complex **6** are low and all of them can be formed.

Diastereoselective Oxidative Addition of EtI, PrI, and BzBr. The reactions of EtI and PrI with **4** are similar and are discussed together (Scheme 4). There are two chief differences from the case of MeI. First, the reactions are much slower and exhibit greater stereoselectivity, as might be expected; only one isomer is observed in each case. Thus, in the case of oxidative addition to **4**, only **8a** or **11a** is formed, indicating essentially exclusive attack above the plane *syn* to the cyclohexyl group. Second, no isomerization is observed to give an isomer with the ethyl or propyl group in the equatorial plane. This feature is readily interpreted in terms of steric effects. Thus, the equatorial site is the most sterically congested, due to interference with the free phenyl substituent of the imine, and there is a high selectivity to place the smallest alkyl group, the methyl group, in this position. This is probably a thermodynamic effect in the present case, though it is also likely that there would be a higher kinetic barrier to isomerization also. The overall result is that the kinetic product forms with the ethyl or propyl group in the axial position and that no subsequent isomerization occurs.

The case of benzyl bromide oxidative addition to **4** can be understood in similar terms (Scheme 4). This reaction is similar in rate to that with MeI and gives similar stereoselectivity in the oxidative addition step, attack occurring mostly *syn* to the cyclohexyl group to give **13a** but with a minor component of attack below the plane to **13b**. No subsequent isomerization occurs, since structures with the benzyl group (as with the ethyl and propyl groups) in the equatorial position are not favored.

The oxidative addition of EtI, PrI, and BzBr to **5** all occur with essentially complete stereoselectivity to give complexes characterized as **9b**, **12b**, and **14b**, respectively (Scheme 3). Since these are thought to have the opposite chirality at platinum compared to the major isomer obtained from MeI and attempts to grow suitable crystals have been unsuccessful, some explanation for the structural assignment is needed. The NMR data show that the methyl group is equatorial but do not distinguish between the isomers **a** and **b**, and the arguments in favor of **b** are as follows. First, it has been established above that CD_3I attacks **5** on the face *anti* to the cyclohexyl group so it is almost certain that this will also be the case with the bulkier alkyl halides. Similarly, it will not be favorable for the bulkier alkyl group to migrate to the sterically congested site in the equatorial plane; therefore no subsequent isomerization is expected to occur. Confirmation is obtained indirectly in the case of EtI addition. Thus, slow hydrolysis of the primary product **9** occurs to give **10**, which has been structurally characterized. Once the bulky free imine group is removed from **9b**, isomerization is possible and the ethyl group migrates to the equatorial site, placing

Scheme 5

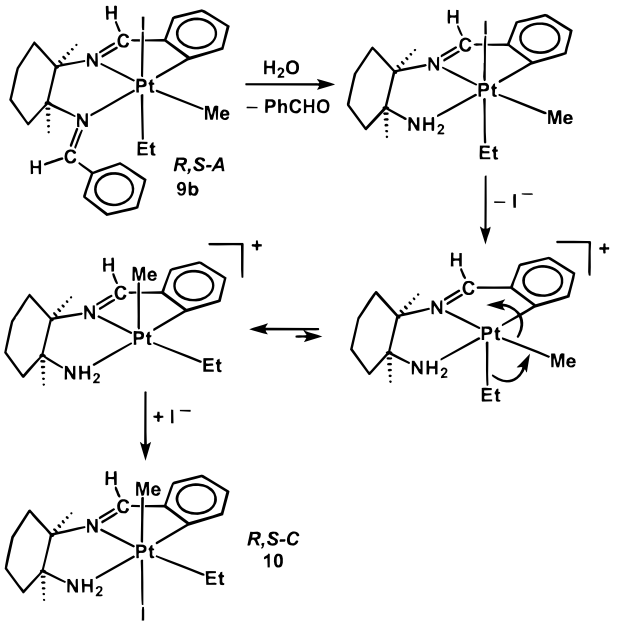

the small methyl group *syn* to the bulky cyclohexyl group. Assuming that the isomerization, like those discussed above, must occur by migration within the meridional plane, the observed structure of **10** then strongly supports the proposed structure of **9b** (Scheme 5).

In conclusion, all of the oxidative additions to **4** and **5** can be understood in terms of the mechanisms shown in Schemes 4 and 3, respectively. The primary oxidative-addition step appears to take place with essentially complete stereoselectivity in all reactions of **5** and in reactions of **4** with ethyl and propyl iodides, though subsequent isomerization can occur easily when R = Me or CD_3 in Schemes 3 and 4. Only in reactions of **4** with MeI, CD_3I, and $PhCH_2Br$ is there evidence for attack at either face of the platinum(II) complex. The combination of asymmetry of the two faces of the platinum(II) complexes, coupled with limitation on the pathways of isomerization due to the presence of the tridentate ligands, has allowed a particularly clear picture of these oxidative-addition reactions to be obtained.

Experimental Section

^{1}H NMR spectra were recorded using a Varian Gemini 300 MHz spectrometer. Chemical shifts are reported relative to TMS. When NOE difference spectra were collected, the percent NOE values were calculated using the equation % NOE = $[(I - I_o)/I]$, where $I - I_o$ is the peak integral in the difference spectrum and I_o is the integral in the spectrum collected with the decoupler frequency set off-resonance. In the NOE difference studies the temperature was controlled at 21 °C, while in the low-temperature studies the sample was cooled using cold nitrogen gas. The molecular mechanics calculations were carried out by using the CAChe software package.[18] The complex $[Pt_2Me_4(\mu\text{-}SMe_2)_2]$ (**3**) was prepared as described previously.[19] All operations were performed under standard Schlenk conditions unless otherwise stated.

Synthesis of Ligands 1 and 2. To a solution of racemic *trans*-1,2-diaminocyclohexane (4 mmol) in diethyl ether (20 mL) was added 2 equiv of benzaldehyde (8 mmol). Excess

(19) Scott, J. D.; Puddephatt, R. J. *Organometallics* **1983**, *2*, 1643.

$MgSO_4$ was added directly to the reaction mixture to remove product water. The solution was stirred for 2 h at room temperature and then filtered. The solvent was removed under vacuum, leaving an off-white residue which was recrystallized from CH_2Cl_2/pentane to give **racemic *trans*-1,2-(N=CHC$_6$H$_5$)$_2$C$_6$H$_{10}$ (1).** Yield: 80%. Anal. Calcd for $C_{20}H_{22}N_2$: C, 82.7; H, 7.6; N, 9.65. Found: C, 82.1; H, 7.8; N, 9.5%. ^{1}H NMR ($CDCl_3$): δ 1.48 [br m, 2H, Cy(H)], 1.82 [br m, 6H, Cy(H)], 3.39 [br m, 2H, Cy(H)], 7.29 [m, 6H], 7.56 [m, 4H], 8.18 [s, 2H, N=CH].

The ligand ***cis*-1,2-(N=CHC$_6$H$_5$)$_2$C$_6$H$_{10}$ (2)** was similarly prepared. Yield: 75%. MS: calcd *m/e* for ($C_{20}H_{22}N_2$ + H^+) 291.1861, found 291.1864. ^{1}H NMR (acetone-d_6): δ 1.63 [br m, 6H, Cy(H)], 2.02 [br m, 2H, Cy(H)], 3.56 [br m, 2H, Cy(H)], 7.38 [m, 6H], 7.72 [m, 4H], 8.29 [s, 2H, N=CH].

Racemic [PtMe{*trans*-1-(N=CHC$_6$H$_4$)-2-(N=CHC$_6$H$_5$)-C$_6$H$_{10}$}] (4). Ligand **1** (0.38 mmol) was reacted with complex **3** (0.19 mmol) in diethyl ether (10 mL). The solution immediately turned orange-yellow which intensified toward orange with time. Within minutes a bright orange solid precipitated. The reaction mixture was stirred overnight (*ca*. 15 h), and the precipitate was filtered off and then washed with diethyl ether (10 mL) and pentane (10 mL). It was then dried under reduced pressure. Yield: 56%. Anal. Calcd for $C_{21}H_{24}N_2Pt$: C, 50.5; H, 4.85; N, 5.6. Found: C, 50.2; H, 4.8; N, 5.45. ^{1}H NMR (CD_2Cl_2): δ 0.51 [s, 3H, ^2J(PtH) = 83 Hz, Pt−Me], 1.47 [br m, 4H, Cy(H)], 1.95 [br t, 2H, Cy(H)], 2.42 [br d, 1H, Cy(H)], 2.56 [br d, 1H, Cy(H)], 3.7 [br t, 1H, Cy(H)], 4.18 [br t, 1H, Cy(H)], 6.98 [t, 1H], 7.18 [t, 1H], 7.42 [m, 4H], 7.56 [t, 1H], 8.27 [d, 2H], 8.64 [d, 1H, ^4J(HH) = 2 Hz, ^3J(PtH) = 61 Hz, N=CH], 8.98 [d, 1H, ^4J(HH) = 2 Hz, ^3J(PtH) = 47 Hz, N=CH].

[PtMe{*cis*-1-(N=CHC$_6$H$_4$)-2-(N=CHC$_6$H$_5$)C$_6$H$_{10}$}] (5) was similarly prepared using the ligand *cis*-1,2-(N=CHC$_6$H$_5$)$_2$C$_6$H$_{10}$ **(2)**. Yield: 55%. Anal. Calcd for $C_{21}H_{24}N_2Pt$: C, 50.5; H, 4.85; N, 5.6. Found: C, 50.1; 4.9; 5.4. ^{1}H NMR (CD_2Cl_2): δ 0.61 [s, 3H, ^2J(PtH) = 84 Hz, Pt−Me], 1.45 [br m, 3H, Cy(H)], 1.90 [br m, 3H, Cy(H)], 2.50 [br d, 1H, Cy(H)], 2.65 [br m, 1H, Cy-(H)], 4.12 [m, 1H, Cy(H)], 4.45 [br s, 1H, Cy(H)], 6.99 [t, 1H], 7.2 [t, 1H], 7.42 [m, 4H], 7.55 [m, 1H], 8.19 [d, 2H], 8.69 [d, 1H, ^4J(HH) = 2 Hz, ^3J(PtH) = 63 Hz, N=CH], 9.02 [s, 1H, ^3J(PtH) = 45 Hz, N=CH].

[PtIMe$_2${*trans*-1-(N=CHC$_6$H$_4$)-2-(N=CHC$_6$H$_5$)C$_6$H$_{10}$}] (6). To an orange solution of complex **4** (0.063 mmol) in THF (10 mL) was added 10 equiv of MeI (0.63 mmol). Within minutes the solution had changed to pale yellow. The reaction mixture was stirred for a total of 90 min, and then the solvent was evaporated under reduced pressure to give a pale yellow solid residue. The residue was recrystallized from a CH_2Cl_2/pentane mixture to give a lustrous yellow powder, which was filtered off and washed with pentane (15 mL). Yield: 78%. Anal. Calcd for $C_{22}H_{27}IN_2Pt$: C, 41.2; H, 4.2; N, 4.4. Found: C, 40.9; H, 4.2; N, 4.3. ^{1}H NMR (CD_2Cl_2): major isomer **6a**, δ 0.67 [s, 3H, ^2J(PtH) = 71 Hz, MePt], 0.78 [s, 3H, ^2J(PtH) = 67 Hz, MePt], 1.40−1.78 [br m, 4H, Cy(H)], 2.05 [m, 2H, Cy(H)], 2.60 [br d, 1H, Cy(H)], 2.75 [br d, 1H, Cy(H)], 3.72 [br t, 1H, Cy-(H)], 4.45 [br t, 1H, Cy(H)], 7.07 [m, 1H], 7.22 [m, 2H], 7.51 [m, 4H], 8.16 [d d, 2H], 8.51 [d, 1H, ^4J(HH) = 2 Hz, ^3J(PtH) = 50 Hz, N=CH], 8.82 [d, 1H, ^4J(HH) = 2 Hz, ^3J(PtH) = 36 Hz, N=CH]; minor isomer **6b**, δ 0.66 [s, 3H, ^2J(PtH) = 72 Hz, MePt], 0.95 [s, 3H, ^2J(PtH) = 66 Hz, MePt], 8.49 [d, 1H, ^4J(HH) = 2 Hz, ^3J(PtH) = 49 Hz, N=CH], 8.96 [d, 1H, ^4J(HH) = 2 Hz, ^3J(PtH) = 36 Hz, N=CH].

[PtIMe$_2${*cis*-1-(N=CHC$_6$H$_4$)-2-(N=CHC$_6$H$_5$)C$_6$H$_{10}$}] (7) was similarly prepared from complex **5**. Yield: 71%. Anal. Calcd for $C_{22}H_{27}IN_2Pt$: C, 41.2; H, 4.2; N, 4.4. Found: C, 40.7; H, 4.0; N, 4.2. ^{1}H NMR (CD_2Cl_2): major isomer **7a**, δ 0.82 [s, 3H, ^2J(PtH) = 72 Hz, MePt], 0.87 [s, 3H, ^2J(PtH) = 66 Hz, MePt], 1.38−2.10 [br m, 8H, Cy(H)], 2.50 [m, 1H, Cy(H)], 4.45 [m, 1H, Cy(H)], 7.08 [m, 1H], 7.22 [m, 2H], 7.50 [m, 4H], 7.86 [d d, 2H], 8.55 [d, 1H, ^4J(HH) = 2.8 Hz, ^3J(PtH) = 49.5 Hz, N=CH], 8.84 [d, 1H, ^3J(PtH) = 34 Hz, N=CH]; minor isomer **7b**, δ 0.65 [s, 3H, ^2J(PtH) = 71 Hz, MePt], 0.87 [s, 3H, ^2J(PtH) = 67 Hz, MePt], 8.51 [d, 1H, N=CH], 8.83 [d, 1H, N=CH].

[PtIMeEt{*trans*-1-(N=CHC$_6$H$_4$)-2-(N=CHC$_6$H$_5$)C$_6$H$_{10}$}] (8). To an orange solution of **4** (0.078 mmol) in THF (10 mL) was added excess EtI (3.88 mmol). The reaction mixture was stirred for 4 h at ambient temperature, during which time the solution changed to yellow. The solvent was evaporated under reduced pressure and the product purified by recrystallization from CH_2Cl_2/pentane. Yield: 96%. Anal. Calcd for $C_{23}H_{29}IN_2Pt$: C, 42.1; H, 4.5; N, 4.3. Found: C, 42.2; H, 4.4; N, 4.1. ^{1}H NMR (CD_2Cl_2): δ 0.27 [t, 3H, ^3J(HH) = 7.8 Hz, ^3J(PtH) = 73.5 Hz, EtPt], 0.74 [s, 3H, ^2J(PtH) = 67.5 Hz, MePt], 1.25 [m, 2H, ^2J(PtH) = 75 Hz, EtPt], 1.40−1.80 [br m, 4H, Cy(H)], 2.0 [m, 2H, Cy(H)], 2.60 [br d, 1H, Cy(H)], 2.75 [br d, 1H, Cy-(H)], 3.72 [br t, 1H, Cy(H)], 4.45 [br t, 1H, Cy(H)], 7.07 [m, 1H], 7.23 [m, 2H], 7.50 [m, 4H], 8.11[br d, 2H], 8.53 [d, 1H, ^4J(HH) = 2 Hz, ^3J(PtH) = 52 Hz, N=CH], 8.88 [d, 1H, ^4J(HH) = 2 Hz, ^3J(PtH) = 39 Hz, N=CH].

[PtIMeEt{*cis*-1-(N=CHC$_6$H$_4$)-2-(N=CHC$_6$H$_5$)C$_6$H$_{10}$}] (9) was similarly prepared from complex **5**. Yield: 83%. Anal. Calcd for $C_{23}H_{29}IN_2Pt$: C, 42.1; H, 4.5; N, 4.3. Found: C, 42.4; H, 4.3; N, 4.0. ^{1}H NMR (CD_2Cl_2): δ 0.25 [t, 3H, ^3J(HH) = 7.5 Hz, ^3J(PtH) = 73 Hz, EtPt], 0.87 [s, 3H, ^2J(PtH) = 67 Hz, MePt], 1.27 [m, 2H, ^2J(PtH) = 75 Hz, EtPt], 1.40−1.64 [br m, 6H, Cy(H)], 1.84 [br m, 2H, Cy(H)], 2.95 [m, 1H, Cy(H)], 4.32 [m, 1H, Cy(H)], 7.06 [m, 1H], 7.21 [m, 2H], 7.42 [m, 1H], 7.53 [m, 3H], 8.14 [br d, 2H], 8.51 [s, 1H, ^3J(PtH) = 52 Hz, N=CH], 8.85 [s, 1H, ^3J(PtH) = 38 Hz, N=CH].

[PtIMeEt{*cis*-1-(N=CHC$_6$H$_4$)-2-(NH$_2$)C$_6$H$_{10}$}] (10). ^{1}H NMR (CD_2Cl_2): δ 0.41 [t, 3H, ^3J(HH) = 7 Hz, ^3J(PtH) = 75 Hz, EtPt], 0.93 [s, 3H, ^2J(PtH) = 72 Hz, MePt], 8.37 [s, 1H, ^3J(PtH) = 44 Hz, N=CH].

[PtIMe(*n*-Pr){*trans*-1-(N=CHC$_6$H$_4$)-2-(N=CHC$_6$H$_5$)-C$_6$H$_{10}$}] (11). To an orange solution of **4** (0.04 mmol) in THF (10 mL) was added excess 1-iodopropane (4.0 mmol). The reaction mixture was stirred for 4 h at ambient temperature. The solvent was evaporated under reduced pressure, yielding a pale yellow residue, which was recrystallized from CH_2Cl_2/pentane to give the product. Yield: 57%. Anal. Calcd for $C_{24}H_{31}IN_2Pt$: C, 43.1; H, 4.7; N, 4.2. Found: C, 43.1; H, 4.6; N, 4.1%. ^{1}H NMR (CD_2Cl_2): δ 0.66 [br m, 3H, Me of PrPt], 0.79 [s, 3H, ^2J(PtH) = 66 Hz, Pt−Me], 1.38−2.75 [br m, 12H, Cy and Pr], 3.65 [br t, 1H, Cy(H)], 4.48 [br t, 1H, Cy(H)], 7.02 [m, 1H], 7.18−7.50 [br m, 6H], 8.08 [m, 2H], 8.47 [s, 1H, ^3J(PtH) = 50 Hz, N=CH], 8.83 [s, 1H, ^3J(PtH) = 39 Hz, N=CH].

[PtIMe(*n*-Pr){*cis*-1-(N=CHC$_6$H$_4$)-2-(N=CHC$_6$H$_5$)-C$_6$H$_{10}$}] (12) was similarly prepared from complex **5**. Yield: 55%. Anal. Calcd for $C_{24}H_{31}IN_2Pt$: C, 43.1; H, 4.7; N, 4.2. Found: C, 43.0; H, 4.6; N, 4.1. ^{1}H NMR (CD_2Cl_2): δ 0.65 [br m, 3H, Me of PrPt], 0.89 [s, 3H, ^2J(PtH) = 67 Hz, Pt−Me], 1.44−1.82 [br m, 12H, Cy and Pr], 2.85 [br m, 1H, Cy(H)], 4.60 [br s, 1H, Cy(H)], 7.06 [m, 1H], 7.22−7.58 [br m, 6H], 8.15 [br d, 2H], 8.51 [s, 1H, ^3J(PtH) = 51 Hz, N=CH], 8.85 [s, 1H, ^3J(PtH) = 38 Hz, N=CH].

[PtBrMeBz{*trans*-1-(N=CHC$_6$H$_4$)-2-(N=CHC$_6$H$_5$)-C$_6$H$_{10}$}] (13). To a solution of **4** (0.04 mmol) in THF (10 mL) was added excess benzyl bromide (4.0 mmol). After 30 min the solution had become pale yellow, and the solvent was evaporated under reduced pressure, giving a yellow oil. The product was crystallized from a CH_2Cl_2/pentane mixture and washed with pentane (15 mL). Yield: 80%. Anal. Calcd for $C_{28}H_{31}BrN_2Pt\cdot 0.5CH_2Cl_2$: C, 48.0; H, 4.5; N, 3.9. Found: C, 48.4; H, 4.5; N, 4.1. ^{1}H NMR (CD_2Cl_2): major isomer **13a**, δ 0.77 [s, 3H, ^2J(PtH) = 66 Hz, MePt], 1.20−1.60 [br m, 4H, Cy-(H)], 1.92 [m, 2H, Cy(H)], 2.36 [br d, 1H, Cy(H)], 2.60 [br d, 1H, Cy(H)], 2.66 [d, 1H, ^2J(H_aH_b) = 9.7 Hz, ^2J(PtH) = 93 Hz, CH_2Bz], 2.87 [d, 1H, ^2J(H_aH_b) = 9.7 Hz, ^2J(PtH) = 102 Hz, CH_2Bz], 3.56 [br t, 2H, Cy(H)], 4.17 [br t, 2H, Cy(H)], 6.59 [m, 2H], 6.94 [m, 2H], 7.02−7.26 [m, 4H], 7.42−7.56 [m, 4H], 7.99

Downloaded by CARLI CONSORTIUM on June 30, 2009
Published on May 23, 1998 on http://pubs.acs.org | doi: 10.1021/om980065z

Table 8. Crystallographic Details

complex	**4**	**7a**	**8a**	**13a**	**10**
empirical formula	$C_{21}H_{24}N_2Pt$	$C_{22}H_{27}IN_2O_{1.5}Pt$	$C_{23}H_{29}IN_2Pt$	$C_{28}H_{31}BrN_2Pt$	$C_{16}H_{25}IN_2Pt$
fw	499.51	665.45	655.47	670.55	567.37
temp, K	298	294	298	297	294
wavelength, Å	0.710 73	0.710 73	0.710 73	0.710 73	0.710 73
cryst syst	orthorhombic	monoclinic	orthorhombic	orthorhombic	triclinic
space group	*Pbca*	$P2_1/c$	*Pbca*	$Pca2_1$	$P\bar{1}$
unit cell dimens					
a, Å	12.629(2)	10.457(2)	15.1691(3)	15.715(2)	9.1339(11)
b, Å	16.374(2)	13.409(2)	15.3153(2)	11.416(3)	9.801(2)
c, Å	17.998(2)	17.048(3)	19.4482(4)	13.603(2)	10.5801(14)
α, deg					81.558(14)
β, deg		104.80 (2)			84.081(10)
γ, deg					70.715(11)
V, Å^3	3721.7(8)	2311.1(7)	4528.2(1)	2440.4(7)	882.8(2)
Z	8	4	8	4	2
calcd density, g cm^{-3}	1.783	1.913	1.927	1.825	2.134
abs coeff, mm^{-1}	7.544	7.423	7.587	7.405	9.689
no. of indep rflns	2563 (*R*(int) = 0.0354)	3391 (*R*(int) = 0.0365)	2915 (*R*(int) = 0.0342)	2430 (*R*(int) = 0.0458)	3108 (*R*(int) = 0.0283)
no. of data/restraints/ params	1417/0/218	3279/0/248	2911/0/244	2400/1/290	2945/0/182
GOF on F^2	1.025	1.073	1.032	1.04	1.014
final *R* indices	R1 = 0.0329	R1 = 0.0395	R1 = 0.0462	R1 = 0.0330	R1 = 0.0350
($I > 2\sigma(I)$)[b]	wR2 = 0.0717	wR2 = 0.1049	wR2 = 0.1013	wR2 = 0.0674	wR2 = 0.0720
R indices (all data)	R1 = 0.0821	R1 = 0.0484	R1 = 0.0622	R1 = 0.0504	R1 = 0.0538
	wR2 = 0.0944	wR2 = 0.1211	wR2 = 0.1106	wR2 = 0.0739	wR2 = 0.0793

[a] GOF = $[\sum w(F_o^2 - F_c^2)^2/(n-p)]^{1/2}$, where *n* is the number of reflections and *p* is the number of parameters refined. [b] $R1 = \sum(||F_o| - |F_c||)/\sum|F_o|$; $wR2 = [\sum w(F_o^2 - F_c^2)^2/\sum wF_o^4]^{1/2}$.

[m, 2H], 8.43 [d, 1H, ^4J(HH) = 3 Hz, ^3J(PtH) = 51 Hz, N=CH], 8.71 [d, 1H, ^4J(HH) = 2 Hz, ^3J(PtH) = 38 Hz, N=CH]; minor isomer **13b**, δ 1.01 [s, 3H, ^2J(PtH) = 66 Hz, MePt], 8.08 [d, 1H, ^4J(HH) = 2 Hz, ^3J(PtH) = 53 Hz, N=CH], 9.06 [d, 1H, ^4J(HH) = 2 Hz, ^3J(PtH) = 37 Hz, N=CH].

[PtBrMeBz{*cis*-1-(N=CHC$_6$H$_4$)-2-(N=CHC$_6$H$_5$)C$_6$H$_{10}$}] (14) was similarly prepared from complex **5**. Yield: 63%. Anal. Calcd for $C_{28}H_{31}BrN_2Pt\cdot 0.5CH_2Cl_2$: C, 48.0; H, 4.5; N, 3.9. Found: C, 47.4; H, 4.5; N, 4.1. ^{1}H NMR (CD_2Cl_2): δ 0.86 [s, 3H, ^2J(PtH) = 66 Hz, MePt], 1.38−1.82 [br m, 6H, Cy(H)], 2.60 [d, 1H, $^2J(H_aH_b)$ = 9 Hz, ^2J(PtH) = 96 Hz, CH_2Bz], 2.62 [m, 1H, Cy(H)], 2.76 [d, 1H, $J(H_aH_b)$ = 9 Hz, ^2J(PtH) = 102 Hz, CH_2Bz], 3.05 [m, 1H, Cy(H)], 3.95 [m, 1H, Cy(H)], 4.30 [m, 1H, Cy(H)], 6.52 [m, 2H], 6.88 [m, 2H], 6.96−7.24 [br m, 4H], 7.34−7.60 [br m, 4H], 7.86 [m, 2H], 8.40 [d, 1H, ^4J(HH) = 2 Hz, ^3J(PtH) = 51 Hz, N=CH], 8.76 [s, 1H, ^3J(PtH) = 37 Hz, N=CH].

X-ray Structure Determination of Complex 4. Red "cube-like" crystals were grown from a mixture of CD_2Cl_2 and pentane, and a crystal of size 0.29 × 0.28 × 0.23 mm was mounted on a glass fiber. The diffraction experiments were carried out using a Siemens P4 diffractometer with the XSCANS software package.[20] The cell constants were obtained by centering 26 high-angle reflections (22.72° ≤ 2θ ≤ 24.93°). A total of 3250 reflections were collected in the θ range 2.26−23.0° (−1 ≤ *h* ≤ 13, −1 ≤ *k* ≤ 18, −1 ≤ *l* ≤ 19) in ω−2θ scan mode at variable scan speeds (2−30 deg/min). An empirical absorption was applied to the data based on the ψ-scan method. SHELXTL programs were used for data processing and the least-squares refinements on F^2.[21] The space group *Pbca* was determined from the systematic absences. All of the non-hydrogen atoms were refined anisotropically. No attempt was made to locate the hydrogen atoms, and they were placed in calculated ideal positions for the purpose of structure factor calculations only. In the final difference Fourier synthesis, the electron density fluctuated in the range from 0.597 to −0.501 e Å^{-3} and the top two peaks were associated with the Pt atom. The maximum shift in the final cycles was 0.001. The experimental details are listed in Table 8, and all positional and thermal parameters, bond distances and angles, anisotropic thermal parameters, and hydrogen atom coordinates and selected torsion angles have been included in the Supporting Information.

X-ray Structure Determination of Complex 7a. Crystals of **7a** were grown from a saturated solution of CH_2Cl_2 layered with pentane. A single crystal suitable for X-ray analysis was mounted inside a glass capillary tube. Data were collected as above. Crystal data and refinement parameters for **7a** are listed in Table 8. The positional and thermal parameters, all bond distances and angles, anisotropic thermal parameters, hydrogen atom coordinates, and selected torsion angles have been included in the Supporting Information. Unit cell parameters were calculated from 25 centered high-angle reflections in the range 15 < 2θ < 25°. Systematic absences were consistent with the monoclinic space group $P2_1/c$. Semiempirical absorption corrections based on ψ-scan data were applied, and full-matrix least-squares refinement on F^2 was performed with anisotropic thermal parameters for all non-hydrogen atoms of the platinum complex. Disordered water molecules (1.5) were modeled in the lattice and refined isotropically with site occupancy factors of 0.65, 0.50, and 0.35. The largest residual electron density peak (1.618 e Å^{-3}) was located between the platinum and iodine atoms.

X-ray Structure Determination of Complex 10. Crystals of **10** were grown from a saturated solution of methylene chloride layered with pentane. A crystal suitable for X-ray analysis was selected and mounted in a glass capillary tube, and data were collected as above. Crystal data and refinement parameters for **10** are listed in Table 8; the positional and thermal parameters, all bond distances and angles, anisotropic thermal parameters, hydrogen atom coordinates, and selected torsion angles have been included in the Supporting Information. A statistical analysis of intensity data indicated the space group $P\bar{1}$. Data were processed, semiempirical absorption corrections based on ψ-scan data were applied, and full-matrix least-squares refinement on F^2 was performed using direct

(20) XSCANS version 2.1; Siemens Analytical X-ray Instruments Inc., Madison, WI, 1994.

(21) SHELXTL Software version 5.0; Siemens Analytical X-ray Instruments Inc., Madison, WI, 1994.

Downloaded by CARLI CONSORTIUM on June 30, 2009
Published on May 23, 1998 on http://pubs.acs.org | doi: 10.1021/om980065z

methods and the SHELXTL program package (version 5.03). All non-hydrogen atoms were refined with anisotropic thermal parameters. The largest residual electron density peak (0.741 e $Å^{-3}$) was associated with the Pt atom.

X-ray Structure Determination of Complex 13a. Crystals of **13a** were grown by slow diffusion from a saturated solution of CH_2Cl_2 layered with pentane. A crystal suitable for X-ray analysis was selected and cut to appropriate size and mounted on a glass fiber. Crystal data and refinement parameters for **13a** are listed in Table 8; the positional and thermal parameters, all bond distances and angles, anisotropic thermal parameters, hydrogen atom coordinates, and selected torsion angles have been included in the Supporting Information. Systematic absences were consistent with the orthorhombic space group *Pbcm* or $Pca2_1$, and the acentric option was chosen and refined successfully. Semiempirical absorption corrections based on ψ-scan data were applied, and full-matrix least-squares refinement on F^2 was performed with anisotropic thermal parameters for all non-hydrogen atoms.

Acknowledgment. We thank the NSERC of Canada for financial support and for a Postgraduate Scholarship to C.R.B.

Supporting Information Available: Tables of X-ray data for complexes **4**, **7a**, **8a**, **10**, and **13a** (32 pages). Ordering information is given on any masthead page.

OM980065Z

Downloaded by CARLI CONSORTIUM on June 30, 2009
Published on May 23, 1998 on http://pubs.acs.org | doi: 10.1021/om980065z